Research Square

Preprints are preliminary reports that have not undergone peer review.
They should not be considered conclusive, used to inform clinical practice,
or referenced by the media as validated information.

Substrate Integrated Waveguide-Based Highly Directive Leaky-Wave Antenna With Pinnate Shaped Slots

Harsh Kumar

harsh.mitp@gmail.com

University School of Information, Communication and Technology, Guru Gobind Singh Indraprastha University

Garima Srivastava

Netaji Subhas University of Technology

Research Article

Keywords: Backward scanning, beam scanning, forward scanning, LWA, SIW

Posted Date: April 22nd, 2026

DOI: https://doi.org/10.21203/rs.3.rs-7211470/v1

License: This work is licensed under a Creative Commons Attribution 4.0 International License.
Read Full License

Additional Declarations: No competing interests reported.

SUBSTRATE INTEGRATED WAVEGUIDE-BASED HIGHLY DIRECTIVE LEAKY-WAVE ANTENNA WITH PINNATE SHAPED SLOTS

Harsh Kumar[1], *Garima Srivastava*[2]

[1]University School of Information, Communication and Technology, Guru Gobind Singh Indraprastha University, New Delhi 110078, India

[2]Department of Electronics and Communication Engineering, Netaji Subhas University of Technology, Delhi 110031, India

Email: [1]harsh.mitp@gmail.com, [2]garima.shrivastav@gmail.com,

Abstract. *In this work, a leaky-wave antenna (LWA) with pinnate-shaped slots and substrate integrated waveguide (SIW) is presented. The suggested antenna design employs eleven periodic slots to increase its gain to 13.1 dB. The antenna exhibits a narrow beamwidth for all scanning frequencies, scanning from forward to backward for frequencies higher than the cut-off frequency. It radiates at −76˚, −30˚, 6˚, 15˚, 20˚, 28˚, 60˚, and 80˚ for frequencies 26.4 GHz, 32.4 GHz, 31.3 GHz, 29.2 GHz, 27.8 GHz, 26.2 GHz, 25 GHz, and 30 GHz, respectively. TE_{10} mode excitation occurs in the proposed SIW-based LWA, in which the antenna leaks the wave through periodic slots embedded in the uppermost layer of SIW. The EM-wave leakage and phase constant can be controlled by varying the slot orientation. The presented LWA is highly directive, with high radiation efficiency and a wide impedance bandwidth (9 GHz) ranging from 25 GHz to 34 GHz. The experimental results of the designed LWA match the simulation results.*

Keywords
Backward scanning, beam scanning, forward scanning, LWA, SIW.

1. Introduction

Leaky-wave antenna (LWA) is a type of traveling-wave antenna designed by loading radiating elements on the transmission line [1]. The first LWA was designed using rectangular waveguide by etching a slot on its top surface [2]. The orientation, shape, and position of the slot decide the polarization and radiation direction of the LWA [3]. The dispersion property of the substrate integrated waveguide (SIW) antenna was presented in [4], demonstrating that a rectangular waveguide integrated on a substrate have the same guided wave characteristics.

The wireless communication systems have undergone extensive development in recent years for developing high-performance antennas. In radar and directional communication systems, narrow beamwidth radiation pattern like a pencil beam and small side lobes at end-fire is required [5−6]. For the end-fire radiation pattern antennas, the phase constant (β) must be equal or greater than its wave number k_0 in the free space. On the other hand, the rectangular waveguides are heavy, bulky and expensive. The polarization and radiation patterns of the conventional LWA were obtained by arranging the slots [7]. LWAs based on SIW technology are gaining popularity due to their low profile, low manufacturing cost, low loss, and ease of integration with planar circuits in lieu of conventional metallic rectangular waveguides [8]. They can produce a narrow beam and scan for different frequencies. SIW comprises of a wide microstrip line shorted with metallic vias at the edges and works as a conventional rectangular waveguide [9]. In [10], a periodic LWA based on SIW was proposed for millimetre-wave applications. In [11], guided wave and mode characteristics of SIW periodic structures were presented and investigated. The theoretical analysis of H-shape slotted SIW antenna was presented in [12]. In [13], an investigation of SIW LWA for narrow beam end-fire radiation and tapered transverse slots was presented. The presented antenna main beam radiates at end-fire, but some side lobe was introduced in it. The authors in [14] developed a half-mode SIW with array of transverse slots, for the applications in microwave and millimetre-wave. In [15], a half mode SIW frequency scanning antenna with multiple

polarizations was investigated. In [16], the authors compared meandering an asymmetrically curved long slot to straight long slot etched on the broadside of straight SIW. In [17], a leaky-wave slotted antenna was discussed for enhancing the beam scanning angle range. A ridged SIW LWA was presented in [18], where side lobe level and cross-polarization can be controlled. In [19], researchers investigated a beam scanning antenna with a composite right- and left-handed transmission line (CRLH TL) structure.

In [20], double-layered vertically stacked SIW LWA exhibited frequency beam steering in the elevation plane and propagation due to the TE_{10} mode excitation of the waveguide. A double-sided LWA [21] produced an asymmetric field on the upper and lower sides of the SIW. The equivalent magnetic currents produced were summed in-phase at the centre of the antenna, increasing its directivity in the E-plane, but fabricating such an antenna was difficult. The channel microstrip line voltage was used to control a dual-band beam scanning LWA at a fixed frequency [22−23]. A planar LWA and array were developed for satellite communication applications [24]. The reported LWA was constructed by etching periodic fan-shaped slots on top of the substrate with SIW technology. The impedance bandwidth of the designed antenna was low; therefore, a non-planar structure was used. A bilateral beam-forming LWA array was investigated [25] for use in indoor and short-distance mobile communications. The antenna array was constructed with a multiport feeding network and a double-layer SIW. A continuous backward-to-forward beam scanning LWA operating in the Ka-band was described in [26]. However, the gain of the antenna was low. A beam scanning LWA using the SIW technique was presented in [27], in which two parallel longitudinal slots of equal length were embedded on the top layer of the rectangular SIW. A SIW LWA for terahertz frequency was designed in [28], with an array of plus sign-shaped slots on the SIW structure. However, the antenna was very large, and it only scanned in the backward direction. In [29], a SIW LWA that is designed on liquid crystal and work on the 30-40 GHz band, but the scanning angle of the antenna was smaller. A slow-wave substrate integrated waveguide (SW-SIW)-based leaky wave antenna (LWA) was demonstrated in[30]. Presented antenna had 8.9 dB gain and 70^0 beam scanning range. A new composite waveguide-based miniature leaky-wave antenna (LWA) that is based on substrate-integrated plasmonic waveguides (SIPW) was presented in[31]and antenna had beam scanning range was from -27° to +62°.

In this article, a LWA antenna using SIW technology is presented, with the designed antenna supporting leaky-wave mode for a large frequency range. In contrast to the proposed antenna, [23] presented an elliptically polarised LWA based on a cross slotted rectangular air-filled waveguide that supports leaky and surface-wave modes. The designed antenna has the advantage of both transverse and longitudinal slot LWA. Using a pinnate slot increases the electrical length of the slot, which increases the path of longitudinal current when compared to a rectangular slot. It enhances the radiation performance and impedance bandwidth of the antenna. A large scanning angle and high gain performance can be obtained by using a pair of slots on the top layer of the SIW as a series loading element.

The EM waves radiate through the periodic slots introduced in the upper layer of SIW, disrupting the current path on the upper layer. The antenna radiates TE_{10}, the dominant mode, from forward to backward as the frequency varies, whereas a rectangular slot antenna scans only forward. By arranging the slot longitudinally and transversely, the current path is increased, and the directivity of the designed antenna improves in comparison to previous work. The LWA scans eight different frequencies from various angles. The unit element of the antenna contains two opposite minor sectors of a circle in place of a circular slot, reducing the antenna's size and displaying circular polarization in the resonating frequency range. The gain and radiation efficiency of the designed antenna are very high.

2. Antenna Design

The slotted SIW LWA with pinnate slot is displayed in Fig. 1. The proposed structure is constructed by introducing two parallel rows of vias that short the parallel conductive planes on a wide microstrip line in the direction of wave propagation. If the distance between the shorting vias in a row is small, the SIW acts like a dielectric-filled conventional rectangular waveguide with transverse slots. This results in a complete planar structure integrated onto a single substrate.

The RT/duroid 5880 substrate with dielectric constant (ε_r) of 2.2 and loss tangent (tan δ) of 0.0009 is used to develop the LWA. The upper surface of the SIW has a series of pinnate-shaped transverse slots with period q etched in them. The structural periodicity is set to one-eleventh of the guided wavelength to avoid multibeam operation [8]. The length, width, and thickness of the designed antenna are represented as L, W, and h, respectively. The width of the SIW is

determined by considering it as a dielectric-filled conventional rectangular waveguide with effective width of w_{eff} [8]. It is calculated by using empirical formulas given in [4], [8]. The diameter and period of vias are denoted as d and s, respectively. The dimensions of the LWA are given in Table 1.

Table 1. Dimensions of the LWA.

Parameter	Value (mm)	Parameter	Value (mm)
L	80	W_1	3.7
W	10.5	W_2	1.6
s	1.5	d	0.5
q	6	θ	64°
r_1	2.1	L_1	4.5
r_2	2.2	L_2	1.05
h	0.5		

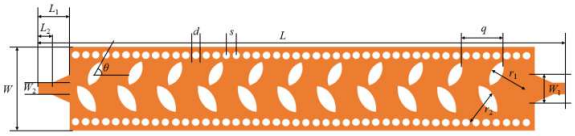


Fig. 1. LWA geometry.

A SIW antenna with a transverse slot works similar to a rectangular waveguide with the transverse slot. Hence, the proposed antenna can be analyzed by transverse slotted SIW rectangular waveguide [7]. The SIW with a pinnate-shaped transverse slot reduces the longitudinal current flowing through the top layer, and the length of the slot edge is longer than that of a rectangular slot, increasing the current density at the slot edge and allowing a large amount of power leakage into space. The leakage current increases in the leaky region as the frequency increases. The leakage constant is nearly zero at the cut-off frequency, where broadside radiation is present [9]. The SIW LWA with transverse slots does not emit at the broadside, therefore the slot in antenna-III is rotated by an angle θ, causing the antenna to emit at the broadside and increasing the scanning angle.

In order to excite the leaky-wave structure, the SIW TE_{10} mode is excited. The proposed structure (antenna-I) behaves as the SIW LWA with a pinnate-shaped transverse slot on the top plane, as shown in Fig. 2(a). Transverse slots are incubated in the upper layer of the SIW to disrupt the distribution of current for power radiation and provide additional phase delay in the transmission line. The unit cell of the LWA is considered as a series combination of transmission line segment loaded impedance and another transmission line. The effective attenuation constant (α_{eff}) and phase constant (β_{eff}) of a unit cell are obtained as,

$$|\beta_{eff}| = \left[\frac{1}{p} Re\left(cos^{-1}\frac{A+D}{2}\right)\right] \quad (1)$$

$$|\alpha_{eff}| = \left[\frac{1}{p} Im\left(cos^{-1}\frac{A+D}{2}\right)\right] \quad (2)$$

where A and D represent the elements of the T parameter matrix of the unit cell.

$$A = D = \left[\frac{1-\left(\left(\frac{Z}{Z_0}\right)^2-1\right)e^{-j2\beta p}}{2+\frac{4}{\frac{Z}{Z_0}}e^{-j2\beta p}}\right] \quad (3)$$

where Z_0 and Z are port impedance and the impedance of the transverse slot, respectively.

$$|\beta_{eff}| = \left[\frac{1}{p} Re(cos^{-1}A)\right] \quad (4)$$

$$|\alpha_{eff}| = \left[\frac{1}{p} Im(cos^{-1}A)\right] \quad (5)$$

In addition, to provide more phase delay in the transmission line, another transverse slot is embedded in the upper layer of SIW (antenna-II), as shown in Fig. 2(b).

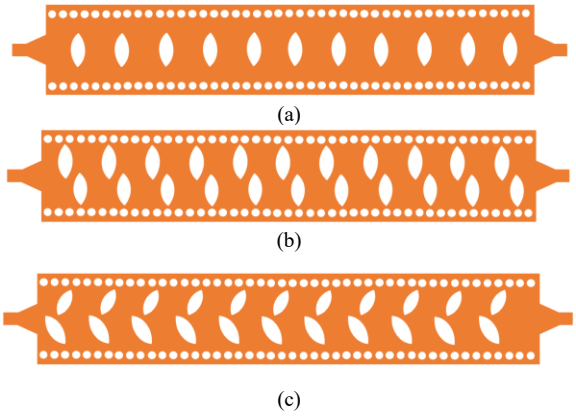


Fig. 2. (a) LWA with transverse slot (antenna-I), (b) LWA with a pair of transverse slots (antenna-II), (c) Proposed LWA (antenna-III).

The equivalent circuit diagram of the antenna to determine input impedance is shown in Fig. 3. Z_1 and Z_2 are the impedances associated with slots one and two, respectively. They are connected in a series as,

$$Z_{eqv} = Z_1 + Z_2 \quad (6)$$

$$A = D = \left[\frac{1-\left(\left(\frac{Z_{eqv}}{Z_0}\right)^2-1\right)e^{-j2\beta p}}{2+\frac{4}{\frac{Z_{eqv}}{Z_0}}e^{-j2\beta p}}\right] \quad (7)$$

The effective attenuation constant and phase constant of the unit cell are shown in Figs. 4 and 5,

respectively. It is clear that TE_{10} excitation occurs in SIW, and the LWA has a cut-off frequency of 10 GHz. When the frequency exceeds 29.8 GHz, the k_0 is lower than the leaky mode phase constant. However, the leaky property of the antenna decreases above this frequency.

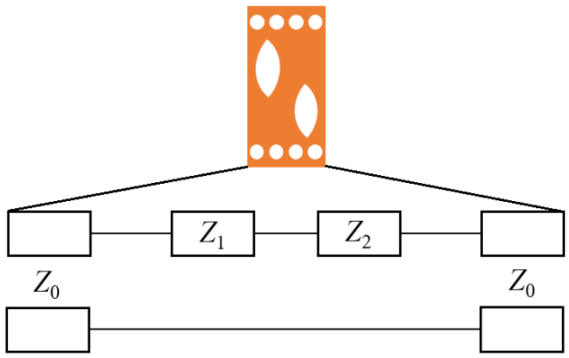


Fig. 3. Equivalent circuit diagram of the unit cell (for antenna-II).

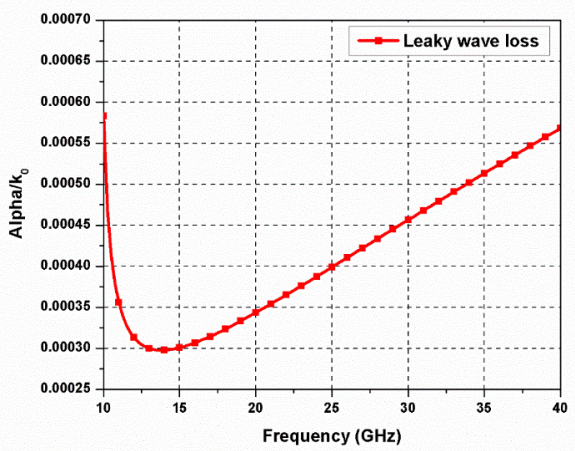


Fig. 4. Normalized attenuation constant in the slotted SIW.

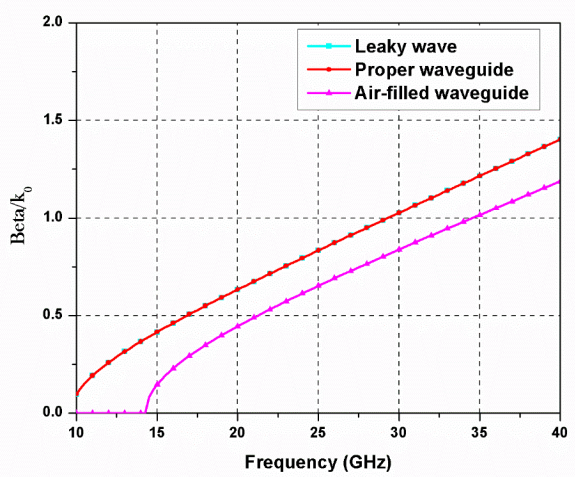


Fig. 5. Normalized phase constant in the slotted SIW.

To achieve circular polarization, a circular slot is required, but it increases the width of the SIW, so the top layer is embedded with two opposite circular sectors of radius equal to a quarter wavelength of the resonant frequency. When an electromagnetic wave enters the unit cell through port 1, any remaining power exits through port 2, resulting in a net electric field pointing from the x-axis to the y-axis. It produced equal magnitude of E_x and E_y, but there is a 90˚ phase difference between them, and the antenna exhibits circular polarization.

Excitation of three modes is possible in the slotted SIW: a leaky-wave mode, which is attenuated and improper; a surface wave mode, which is properly bound; and, a normal waveguide mode. The radiation mechanism of LWA can be explained by complex longitudinal propagation constant of leaky wave mode [9],

$$\beta = \sqrt{\varepsilon_r k_0^2 - \left(\frac{\pi}{w_{eff}}\right)^2} \tag{8}$$

where β represents the phase constant, ε_r represents the relative permittivity of the substrate, w_{eff} is the effective width of the SIW antenna, and α is the leakage rate of the SIW for TE_{10} mode. The radiated power of the antenna varies with the leakage rate (α) and length (L) of the LWA. Fig. 6 shows the dispersion diagram of two transverse slots and the proposed antenna. As shown in Fig. 2(b), one more transverse slot is embedded on the top layer of SIW to improve the performance of the antenna. It is used to provide series radiator slots and make optimization easy.

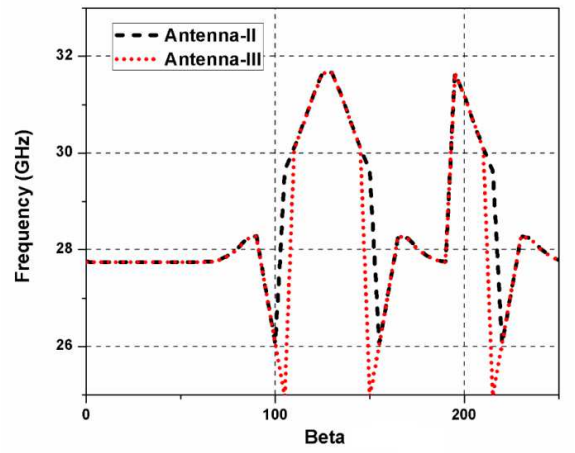


Fig. 6. Dispersion diagrams of the proposed antenna.

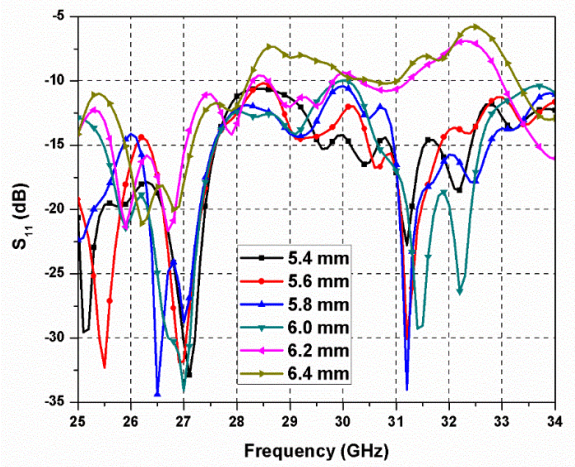


Fig. 7. Reflection coefficients of the antenna on varying the distance between slots.

3. Results and Discussion

The stopband at transition frequency can be suppressed by properly arranging the slot, so the LWA radiates a broad range of frequencies. With the help of parametric analysis, the dimensions of the unit cell can be optimized. In Fig. 7, the period of the slot (q) is varied and it is observed that at q = 6 mm and θ = 26°, the stop band is completely suppressed and return loss is lower than −10 dB for the entire band.

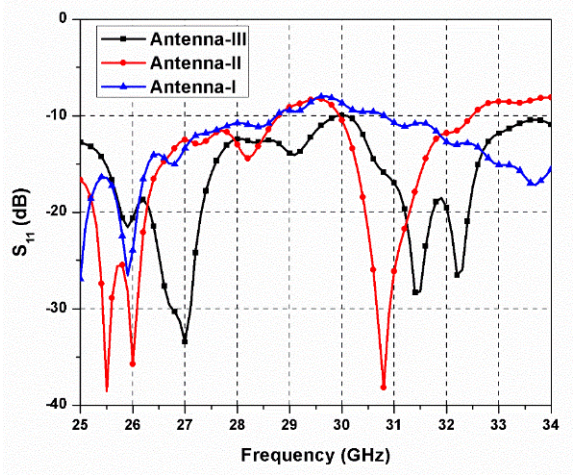


Fig. 8. S-parameters of the SIW LWA configurations.

Fig. 8 represents the reflection coefficients of the LWA configurations. Antenna designs with a single transverse slot and two transverse slots have a stop band at 29 to 30 GHz. However, the stop band tendency can be suppressed by arranging the slots properly, and S_{11} for antenna-III is below −10 dB across the frequency range. Fig. 9 shows simulated S-parameters (S_{11}, S_{22}, and S_{21}) of the antenna-III.

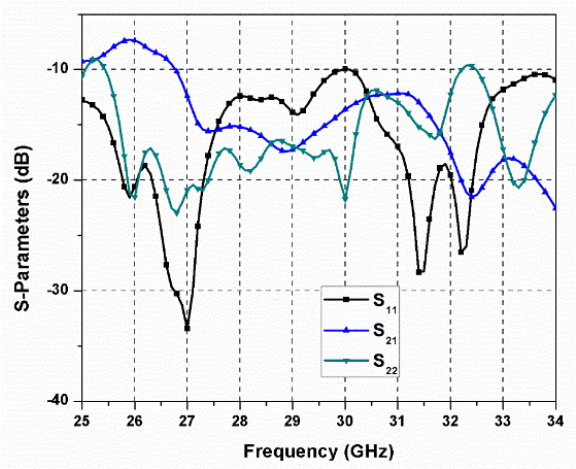


Fig. 9. S-parameters of the antenna-III.

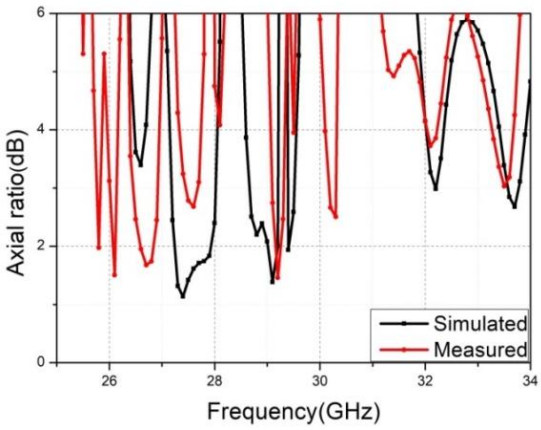
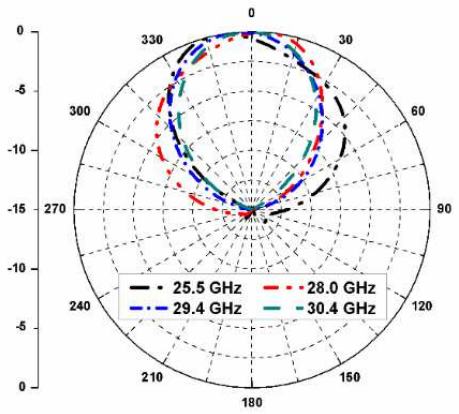


Fig. 10. Axial ratio of the antenna-III.

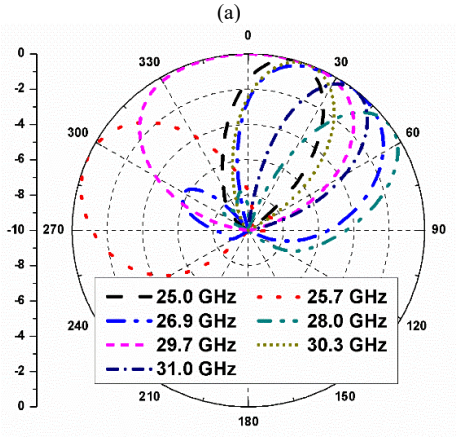
Fig. 10 shows the axial ratio of the antenna, which is less than 3 dB at 26.7 GHz. Therefore, the antenna exhibits circular polarization in the 26.7 GHz frequency range. The radiation patterns of antenna-I are depicted in Fig. 11(a). The antenna has no scanning property, radiates from the broad side, and has a very large beamwidth.

Fig. 11(b) depicts the radiation patterns of antenna-II. This antenna radiates at different angles depending on the frequency. It radiates at −75°, 0°, 15°, 25°, 40°, and 55° at frequencies of 25.7 GHz, 29.7 GHz, 25 GHz, 26.9 GHz, 31 GHz, and 28.6 GHz, respectively. The antenna shows beam scanning property, but its beamwidth is very high. Furthermore, to improve the scanning property and beamwidth, the orientation of the slots is changed, and Fig. 11(c) depicts the radiation patterns of antenna-III, which exhibits beam scanning property with a narrow beamwidth similar to a pencil beam. The antenna radiates at −76°, −30°, 6°, 15°, 20°, 28°, 60°, and 80° GHz for frequencies of 26.4 GHz, 32.4 GHz, 31.3 GHz, 29.2 GHz, 27.8

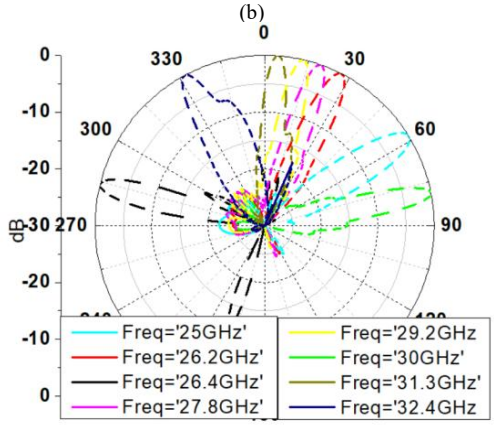
GHz, 26.2 GHz, 25 GHz, and 30 GHz, respectively.



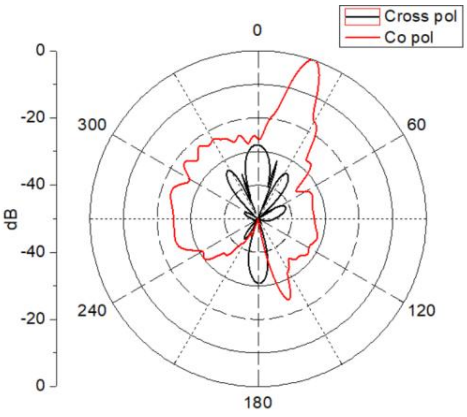
(a)



(b)

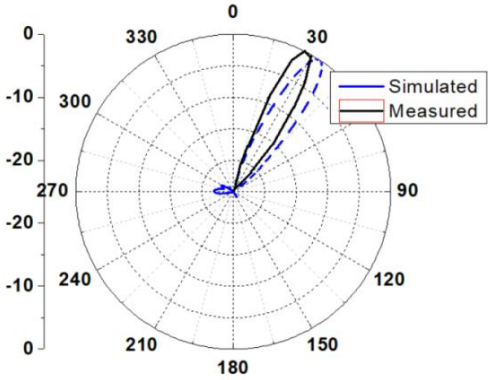


(c)

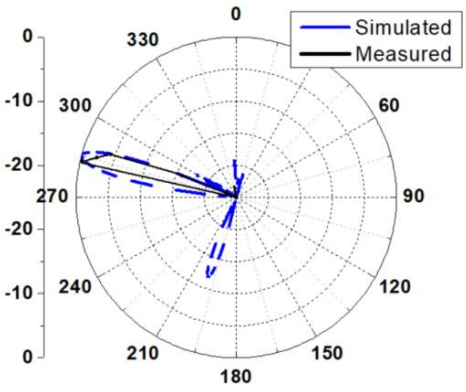


(d)

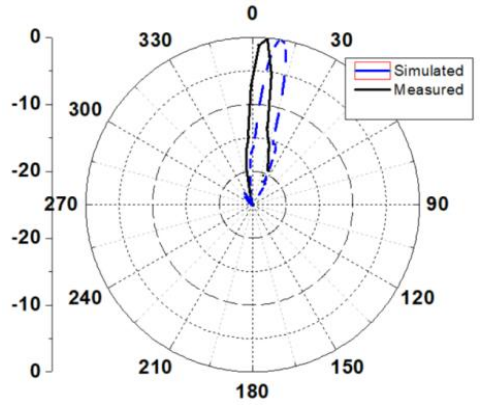
Fig. 11. Radiation patterns of the SIW LWA: (a) Antenna-I, (b) Antenna-II, (c) Antenna-III, (d) Co- and cross-polarization at 27.8 GHz.



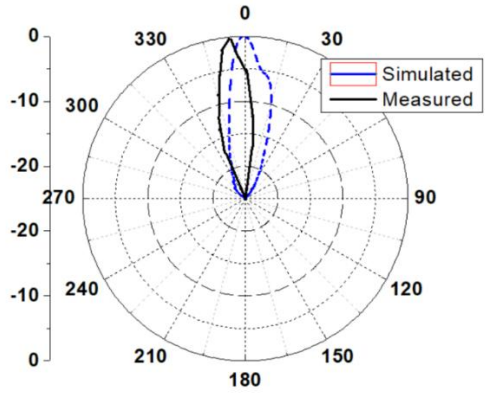
(a)



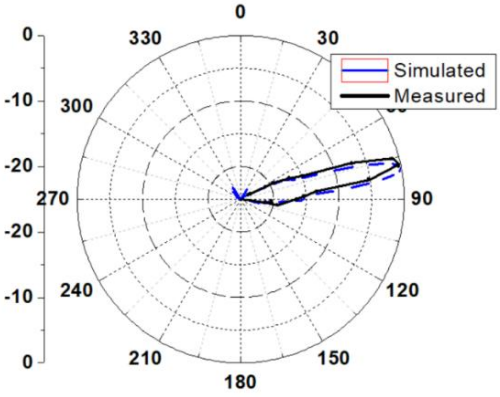
(b)



(c)



(d)



(e)

Fig. 12. Simulated and measured radiation patterns of the antenna-III: (a) 26.2 GHz, (b) 26.4 GHz, (c) 29.2 GHz, (d) 31.1 GHz, (e) 30 GHz.

A few side lobes are also visible, which could be due to surface wave mode propagation. This mode is used when the wave number in a dielectric medium exceeds the wave number in free space. Surface waves generate side lobes that radiate in the near end-fire direction.

The fabricated prototype of the proposed LWA is presented in Fig. 13. The radiation patterns of antenna-III at different frequencies are shown in Fig. 12. Antenna scans in backward direction −76˚ to forward direction +80˚. The small difference between measured and simulated results is due to mutual coupling of current from the slot's tip. The simulated and measured reflection coefficients of the antenna-III are presented in Fig. 13. In both simulated and measured results, the antenna shows a dip at 27 GHz, 29 GHz, and 32.5 GHz.

The simulated and measured gain plots of the presented antenna are given in Fig. 14. The gain curves are approximately the same in both cases. A small mismatch between the measured and simulated results is due to fabrication defect, measurement error, and SMA connector losses. Due to the small value of attenuation constant, the proposed antenna transmits maximum power at the output part. Fig. 15 shows the radiation efficiency of the designed antenna, which varies from 94% to 97% for the entire frequency range.

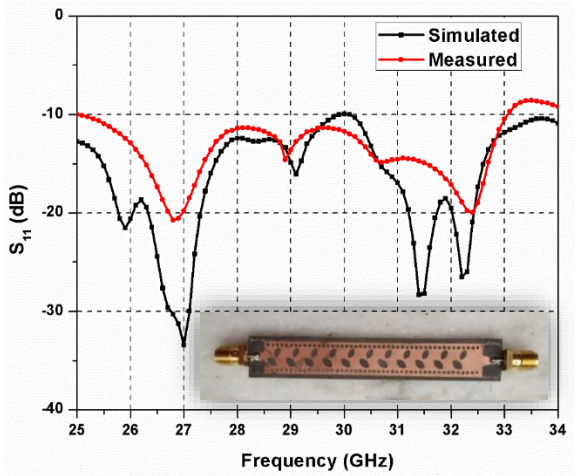


Fig. 13. Simulated and measured reflection coefficients of the antenna-III.

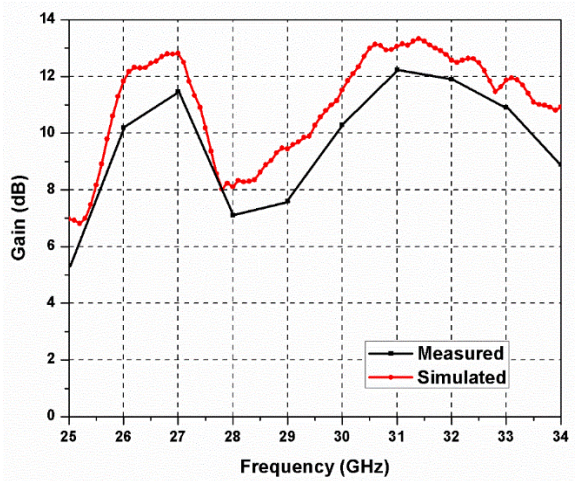


Fig. 14. Simulated and measured gain of the antenna-III.

The performance of the proposed antenna is compared to previous works in Table 2. The reported

antenna designs had used longitudinal or transversal slots on the top layer of the SIW, with longitudinal slots radiating broadside and transverse slots radiating in end-fire direction. Whereas, the proposed antenna-III consisted of a pair of leaf-shaped slots that are 64˚ degrees apart. The antenna radiates end-fire in the broadside direction, and scans forward and backward through the broad side.

The suggested antenna has been compared with recent work in the comparison table. The suggested antenna has a broad impedance bandwidth, which is 9.5 GHz. In [25], [29], the impedance bandwidth is somewhat greater than that of the proposed antenna, although these antennas are roughly twice as large as the proposed antenna. In comparison to other designs, the proposed antenna has a low beamwidth of 130 and a high gain of 13.1 dB. In contrast to the suggested design's 10 unit cells, the antennas in [25] and [27] used 20 unit cells. In contrast to prior designs, the suggested concept has a high beam scanning range and a very small dimension.

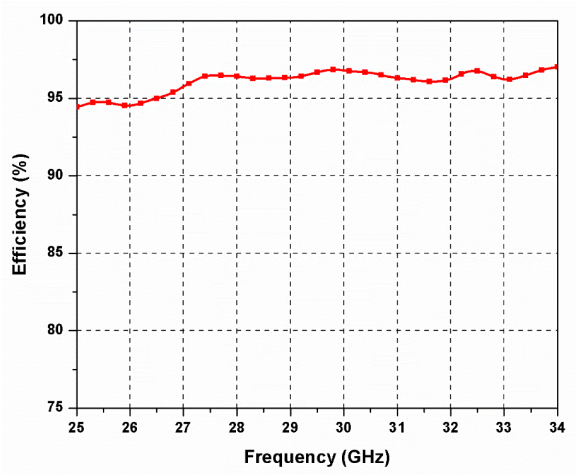


Fig. 15. Radiation efficiency of the designed antenna-III.

Table 2. Comparison of the proposed antenna with existing antenna designs.

Ref.	Frequency (GHz)	Impedance bandwidth (GHz)	Polarization	Gain (dBi)	Beamwidth (in degree)	Structure	Beam scanning angle	Size
[24]	28	27.4−28.5 (1.1)	Linear	4.52	26˚	Planar	−45˚ to +45˚	---
[25]	28	27.4−37.3 (9.9)	Circular	16.5	---	Non planar	0˚ to +51˚	---
[26]	34	32−36 (4)	Linear	9.1	45˚	Planar	−56˚ to +48˚	78 × 47
[27]	14	10−18.22 (8.22)	Linear	14.5	15˚	Planar	−58˚ to +59˚	184 × 16
[28]	106	105−109 (4)	Linear	12.33	---	Planar	−6˚ to +76˚	147 × 16
[29]	34.7	30−40 (10)	Linear	12.63	20˚	Planar	−53˚ to 60˚	---
This work	28	24.5−34 (9.5)	Circular	13.1	13˚	Planar	−76˚ to +80˚	80 × 10.5

4. Conclusion

The designed antenna is comprised of transverse and longitudinal slots and scans continuously in the forward and backward directions at different frequencies. The presented SIW-based LWA with asymmetric pairs of slots on the dielectric-filled rectangular waveguide results in the extraction of narrow beamwidth. The advantage of both longitudinal and transverse slots may be obtained by adding inclined slots to the upper layer of the leaky wave guided structure. Additionally, a wide range of beam scanning capabilities can be accomplished by adjusting the rotational angle. By adding more periodic slots, the antenna's gain and efficiency can be increased. The proposed LWA is simple, comparable in size with an array, and does not need complex feeding. An impedance bandwidth of 25 to 34 GHz is obtained. The realized gain of the designed antenna varies from 8 to 13.1 dB. It radiates broadside to near end-fire direction with 96% radiation efficiency. Good compliance is achieved between simulated and experimental results.

References

[1] Oliner A A and Jackson David R, 2007 Antenna Engineering Hand Book, 4th ed., New York: McGraw Hill.

[2] Hyneman R. 1959 Closely-spaced transverse slots in rectangular waveguide. IRE Transactions on Antennas and Propagation 7.4: 335-342.

[3] Juhua Liu, Jackson David R., and Long Yunliang. 2011 Modal analysis of dielectric-filled rectangular waveguide with transverse slots. IEEE Transactions on antennas and propagation 59.9: 3194-3203.

[4] Cassivi Y, Perregrini L, Arcioni P, Bressan M, Wu K, Conciauro G. 2002 Dispersion characteristics of substrate integrated rectangular waveguide. IEEE Microwave and Wireless Components Letters. 12(9):333-5.

[5] Wang J, Geng Y, Wang J. 2016 Low-sidelobe non-uniform transverse slotted antenna array fed by substrate integrated waveguide. IEEE International Conference on Microwave and Millimeter Wave Technology 2: 817-818.

[6] Geng Y, Wang J, Li Y, Li Z, Chen M, Zhang Z. 2017 High-efficiency leaky-wave antenna array with sidelobe suppression and multibeam generation. IEEE Antennas and Wireless Propagation Letters. 29;16: 2787-90.

[7] Liu J, Jackson DR, Long Y. 2011 Substrate integrated waveguide (SIW) leaky-wave antenna with transverse slots. IEEE Transactions on Antennas and Propagation. 15;60(1): 20-9.

[8] Xu F, Wu K. 2005 Guided-wave and leakage characteristics of substrate integrated waveguide. IEEE Transactions on microwave theory and techniques. 17;53(1): 66-73.

[9] Lyu YL, Liu XX, Wang PY, Erni D, Wu Q, et. al. 2016 Leaky-wave antennas based on non cut off substrate integrated waveguide supporting beam scanning from backward to forward. IEEE Transactions on Antennas and Propagation. 4;64(6): 2155-64.

[10] Xu F, Wu K, Zhang X. 2009 Periodic leaky-wave antenna for millimeter wave applications based on substrate integrated waveguide. IEEE

Transactions on Antennas and Propagation. 30;58(2): 340-7.

[11] Lyu YL, Meng FY, Yang GH, Erni D, Wu Q, Wu K. 2017 Periodic SIW leaky-wave antenna with large circularly polarized beam scanning range. IEEE Antennas and Wireless Propagation Letters. 12;16: 2493-6.

[12] Liu J, Tang X, Li Y, Long Y. 2012 Substrate integrated waveguide leaky-wave antenna with H-shaped slots. IEEE transactions on antennas and propagation. 23;60(8): 3962-7.

[13] Liu J, Jackson DR, Li Y, Zhang C, Long Y. 2014 Investigations of SIW leaky-wave antenna for end fire-radiation with narrow beam and sidelobe suppression. IEEE Transactions on antennas and Propagation. 25;62(9): 4489-97.

[14] Lai QH, Hong W, Kuai ZQ, Zhang YS, Wu K. 2009 Half-mode substrate integrated waveguide transverse slot array antennas. IEEE Transactions on Antennas and Propagation. 7;57(4): 1064-72.

[15] Cheng YJ, Hong W, Wu K. 2010 Millimeter-wave half mode substrate integrated waveguide frequency scanning antenna with quadri-polarization. IEEE Transactions on Antennas and Propagation. 29;58(6): 1848-55.

[16] Cheng YJ, Hong W, Wu K, Fan Y. 2010 Millimeter-wave substrate integrated waveguide long slot leaky-wave antennas and two-dimensional multibeam applications. IEEE Transactions on Antennas and Propagation. 1;59(1): 40-7.

[17] Kim DJ, Lee JH. 2013 Beam scanning leaky-wave slot antenna using balanced CRLH waveguide operating above the cutoff frequency. IEEE transactions on antennas and propagation. 4;61(5): 2432-40.

[18] Mallahzadeh A, Mohammad-Ali-Nezhad S. 2014 Long slot ridged SIW leaky wave antenna design using transverse equivalent technique. IEEE Transactions on Antennas and Propagation. 4;62(11): 5445-52.

[19] Cao W, Chen ZN, Hong W, Zhang B, Liu A. 2014 A beam scanning leaky-wave slot antenna with enhanced scanning angle range and flat gain characteristic using composite phase-shifting transmission line. IEEE Transactions on Antennas and Propagation. 21;62(11): 5871-5.

[20] Monavar FM, Shamsinejad S, Mirzavand R, Melzer J, Mousavi P. 2017 Beam-steering SIW leaky-wave subarray with flat-topped footprint for 5G applications. IEEE transactions on antennas and propagation. 1;65(3):1108-20.

[21] Martinez-Ros AJ, Bozzi M, Pasian M. 2018 Double-sided SIW leaky-wave antenna with increased directivity in the $ E $-plane. IEEE Transactions on Antennas and Propagation. 5;66(6):3130-5.

[22] Wang M, Ma HF, xuan Tang W, Zhang HC, xiang Jiang W, Cui TJ. 2019 A dual-band electronic-scanning leaky-wave antenna based on a corrugated microstrip line. IEEE Transactions on Antennas and Propagation. 4;67(5):3433-8.

[23] Liu J, Long Y. 2012 A full-wave numerical approach for analyzing rectangular waveguides with periodic slots. IEEE Transactions on Antennas and Propagation. 23;60(8): 3754-62.

[24] Li X, Wang J, Li Z, Li Y, Geng Y, Chen M, et. al. 2021 Leaky-wave antenna array with bilateral beamforming radiation pattern and capability of flexible beam switching. IEEE Transactions on Antennas and Propagation. 15;70(2):1535-40.

[25] Li X, Wang J, Goussetis G, Wang L. 2022 Circularly polarized high gain leaky-wave antenna for CubeSat communication. IEEE Transactions on Antennas and Propagation. 21;70(9):7612-24.

[26] Xu K, Wang Q, Lv L, Zhang Q, Sun S, Luo F, Luo Xe, et. al. 2022 SIW-Based-Band Leaky-Wave Antenna With Improved Beam Steering Performance. IEEE Antennas and Wireless Propagation Letters.1:21(11) 2224-8.

[27] Arya, V., Garg, T., & Al-Khafaji, H. M. R. (2023). High gain and wide-angle continuous beam scanning SIW leaky-wave antenna. Electronics, 12(2), 370.

[28] Arya, V., Garg, T., & Al-Khafaji, H. M. R. (2023). SIW leaky wave antenna for THz applications. Electronics, 12(8), 1839.

[29] Hou S, Fang S, Wang Y, Wang M, Wang Y, Tian J, Feng J. A Ka-band one-dimensional beam scanning leaky-wave antenna based on liquid crystal. Sci Rep. 2024 Feb 16;14(1):3937. doi: 10.1038/s41598-024-54688-4. PMID: 38366014; PMCID: PMC10873358.

[30] Jia-Yuan Yin, Peng-Ye Li, and Jing-Ya Deng, "Circularly polarized beam-scanning leaky wave antenna based on a slow-wave substrate integrated waveguide," Appl. Opt. 63, 5440-5445 (2024).

[31] Liming Si, Kunlin Han, Rong Niu, Lin Dong, Wentao Xing, and Weiren Zhu, "Miniaturized leaky-wave antenna with backward-to-forward beam scanning and suppressed open stop-band based on substrate-integrated plasmonic waveguide," Opt. Express 32, 19352-19360 (2024)



Harsh Kumar was born in year 1984, obtained his B.Tech in Electronics and Communication Engineering from MIT Purnea in 2008 and M.Tech degree in Microwave Engineering From BIT Mesra, Ranchi, India in the year 2010. He has completed his Ph.D. degree in Electronics and communication engineering, Guru Gobind Singh Indraprastha University, Delhi, India in March 2025. He has authored/co-authored several research papers in referred International Journals and Conferences. His research has included microwave communications, planar and conformal microstrip antennas including array mutual coupling, DGS, novel antennas, UWB antennas, SIW Antenna, numerical methods in electromagnetic and composite right/left handed (CRLH) transmissions. His skill includes modeling of antenna and RF circuits with Ansoft HFSS/ADS Momentum, measurements using Vector Network Analyzer and Anechoic Chamber.



Garima Srivastava received her B.Tech degree in Electronics and Communication from J.K Institute Allahabad University, India in 2000 and M.Tech degree in Electronics from J.K Institute Allahabad University in 2002.She is working as an Assistant Professor in Ambedkar Institute of Advanced Communication Technologies and Research since 2011.She is a senior member of IEEE .She has chaired IEEE conferences and also been technical programme committees of various conferences. She has been teaching courses on Microwave Engineering, Antenna and Wave Propagation, Analog Electronics, Wireless Communication, Smart Antennas. She received her PhD degree in Electronics from SHIATS institute, Naini Allahabad deemed to be University. Her research interest includes RF and Microwave Engineering, Antenna Designing, Wireless Communication, Internet of Things.